

Positional and Force Characteristics of neuroArm Robotic Manipulators: A Pilot Study

Yaser Maddahi, Kouros Zareinia, Liu Shi Gan, Sanju Lama, Garnette R. Sutherland

Project neuroArm, Department of Clinical Neuroscience, University of Calgary
3280 Hospital Dr NW, Calgary, AB T2N 4Z6.
ymaddahi@ucalgary.ca; kzareini@ucalgary.ca; lsgan@ucalgary.ca; slama@ucalgary.ca;
garnette@ucalgary.ca

Nariman Sepehri

Department of Mechanical Engineering, University of Manitoba
75A Chancellor Circle, Winnipeg, MB R3T 5V6.
nariman.sepehri@umanitoba.ca

Abstract- A prerequisite for the successful design of the hand-controller, an important element of a tele-surgical robotic system, remains i) the knowledge of the forces exerted by the surgical tool, and ii) the workspace required to maneuver the tool during surgical procedures. In this study, we used an image-guided neurosurgical telerobotic system called neuroArm, to quantify both the forces of tool tissue interaction and the workspace of the surgical tool attached at the two end-effectors. neuroArm includes two manipulators to which different surgical tools can be attached; in this particular study a bipolar forceps on the right and a suction tool on the left. The position, orientation, and force exerted by each tool were measured during the removal of a brain tumour, a grade III oligoastrocytoma. It was shown that the force applied by the bipolar forceps was more than that by the suction. Furthermore, the position, orientation and force of the forceps (with higher SEM) were more oscillatory than that of the suction tool (with less SEM). Results, obtained in this pilot study, can be further strengthened by the inclusion of multiple surgical procedures. This will provide a better understanding of the tool-tissue interaction in robot-assisted microsurgical systems.

Keywords: Robot-assisted surgery, neuroArm surgical system, workspace, tool-tissue interaction force.

1. Introduction

Robotic systems in neurosurgery have the potential of enhancing surgical performance by increasing accuracy, precision, and safety of surgery. Only a few telesurgical robotic systems have been developed and/or commercialized to date, each with its unique technical specifications (Mitsubishi *et al.*, 2013; Arata *et al.*, 2011; Comparet *et al.*, 2011; Hongo *et al.*, 2006; Goto *et al.*, 2009). When coupled to image-guidance, such systems offer several advantages over conventional surgery such as navigating the tool through narrow surgical corridors, eliminating the problem of brain shift, achieving optimal resection control, and reducing surgeon fatigue (Sutherland *et al.*, 2015). Furthermore, such systems can provide a platform for case documentation, safety, and education (Zareinia *et al.*, 2015). These will become increasingly integrated into neurosurgical practice as advances in technology, machine control, and computer processing occur (Camarillo *et al.*, 2004).

There are a few robot-assisted surgical systems capable of microsurgery. Two of these systems that were prototyped at Nagoya University (Mitsubishi *et al.*, 2013) and University of Tokyo (Arata *et al.*, 2011) lack haptic interface, and three include haptics: neuroArm (Sutherland *et al.*, 2008a), ROBOCAST (Comparet *et al.*, 2011) and NeuRobot (Hongo *et al.*, 2006). None of these five systems are commercially

available. Both NeuRobot and neuroArm have been used in patients, and only neuroArm is presently being used in clinical studies (Sutherland *et al.*, 2008b; Sutherland *et al.*, 2013). To date, the system has been used in 56 cases, primarily for CNS neoplasia and cavernous angioma (18 Glioma, 27 meningioma, 4 cavernous angioma, and 8 other cases).

Sensory immersive workstation of the neuroArm allows the surgeon to interact with imaging data without interrupting the rhythm of surgery. However, the existing hand-controller is not specifically designed for neurosurgery, but a multi-purpose commercial product (Omega 7, Force Dimension, Switzerland) that is integrated into the system. The authors believe that a hand-controller that is built based on data obtained from actual neurosurgical procedures will allow optimization of workspace, force feedback and usability for neurosurgery. As the first step, variations of positional displacements of surgical tools and the forces exerted by surgeons were measured during a case of robot-assisted neurosurgery, as both positional and force data are prerequisites to design such a system for microsurgery (Marcus *et al.*, 2014). Measuring workspace and force needs an instrumented platform to continually record the required data (Gonzalez-Martinez *et al.*, 2014; Sutherland *et al.*, 2008a; Haidegger *et al.*, 2008; Shoham *et al.*, 2006). An approach to collect the required information is to use an instrumented surgical robotic system to record positional and force data during surgery, which is not possible in conventional surgery. In this paper, we used neuroArm surgical system to report the workspace of two surgical tools attached to the end-effectors, and their interaction forces with the brain tissue. The workspace and force were quantified by analyzing data from a grade III oligoastrocytoma case. This work is a preliminary study that will be extended to obtain the forces exerted and workspace for multiple surgical procedures and tasks. The data can also be used for quality assurance and case rehearsal which may be of value, particularly in training of a novice surgeon and help to make the initial experience with robotic surgery safer, less stressful, and more efficient (Sutherland *et al.*, 2015).

The rest of this paper is organized as follows. Section 2 presents an overview of the neuroArm surgical manipulator mechanism and working procedure. Section 3 presents the test procedure. Results are shown in Section 4, followed by conclusions in Section 5.

2. Experimental Setup

2. 1. Robotic Manipulators (Arms)

neuroArm is an MR compatible, image-guided robotic system (Fig. 1) capable of microsurgery and stereotaxy. Each arm has 6 degrees-of-freedom (DOFs) including shoulder yaw, shoulder roll, elbow yaw, elbow roll, wrist pitch, tool roll and tool actuation. neuroArm comprises two robotic manipulators with their own surgical tool installed at each end-effector (Fig. 1c). The manipulators are mounted on a mobile base which provides the system better movability. Each manipulator is controlled with a haptic device located in a sensory-immersive workstation (Fig. 2). The surgeon is seated in the workstation and moves the hand-controller, and uses the pair of hand-controllers. Commands of the haptic devices are transferred to the operation room through Local Area Network (LAN) with no packet loss and time delay (Maddahi *et al.*, 2013). Two Titanium Nano17 force sensors (ATI Technologies Inc.) are attached to each end-effector to measure the interaction forces between the surgical tool and the brain tissue. Measured forces are relayed to the remote surgeon in real-time via the haptic hand-controllers at the workstation.

2. 2. Workstation

The workstation, shown in Fig. 2, include: a pair of Omega 7 haptic devices (Force Dimension, Switzerland), two 24" medical grade HD displays for MRI imaging and stereoscopic view of the surgical field (LMD 2450 MD; Sony, Japan), a 15" touch-screen monitor for graphical user interface and command status display (Elo Touch Solutions, CA, US), and a pair of foot pedals that activate and deactivate manipulation movements. Omega 7 introduces 7 positional sensing DOFs (3 translations, 3 rotations and 1 for gripper) and 3+1 force DOFs: 3D active force feedback, and 1 active grasping. It is also capable of producing force up to 12 N and grasping force feedback up to 8 N. The touch screen displays the neuroArm manipulator orientation and the graphical user interface (GUI). Stereoscopic vision of the surgical field is

provided via the 3D display mounted at the centre of the workstation. The monitor is connected to two HD microscope cameras (PMW- 10MD, Sony, Japan) that are mounted on the surgical microscope. An additional display is connected to the environment awareness field camera which allows the remote surgeon to view the environment surrounding the manipulators to avoid accidental collision with the surrounding surgical instrument, objects, or OR personnel.

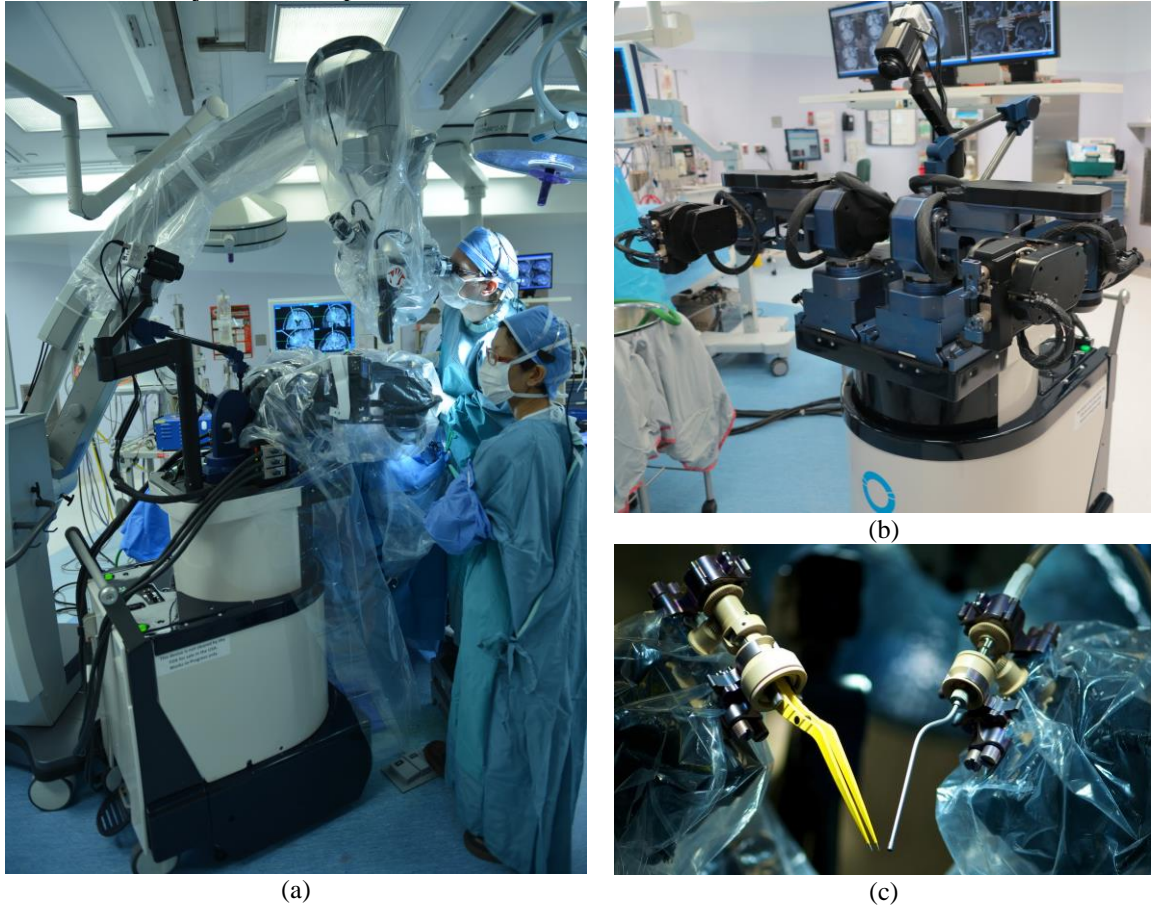


Fig. 1. (a) neuroArm manipulator located inside the operating room (OR) at Foothills Hospital, Calgary, Alberta, Canada; (b) neuroArm surgical manipulators; (c) bipolar forceps and suction tools attached to the right and left manipulator, respectively.



Fig. 2. Surgeon utilizes a pair of Omega 7 haptic devices to guide the neuroArm manipulator. Each haptic device provides information to one of the manipulators.

2. 3. Clinical Setup

Figure 3 shows the schematic details of the neuroArm system together with its integration into the 3.0 T iMRI operating suite at Foothills Hospital, Calgary, Alberta, Canada. The sensory immersive workstation is located in an adjacent room (control room) next to the iMRI operating suite (see Fig. 2). The manipulators are connected to the main system controller via a junction box that is located beneath the foot-end of the OR table. For microsurgery, both surgical microscope and the neuroArm manipulators are positioned by the cranial end of patient, and are oriented relative to the side and location of the surgical opening. The surgical team typically consists of the main surgeon, the assistant surgeon, anaesthesiologist, scrub nurse, circulating nurse, and dedicated neuroArm robot technician(s) or engineer. Setup and start-up testing of the neuroArm system are typically performed in tandem with patient preparation and wound. Once setup is completed, the sterile scrub nurse will perform draping of the neuroArm manipulators and surgical microscope, along with attachment of the sterile tool holders and surgical instruments.

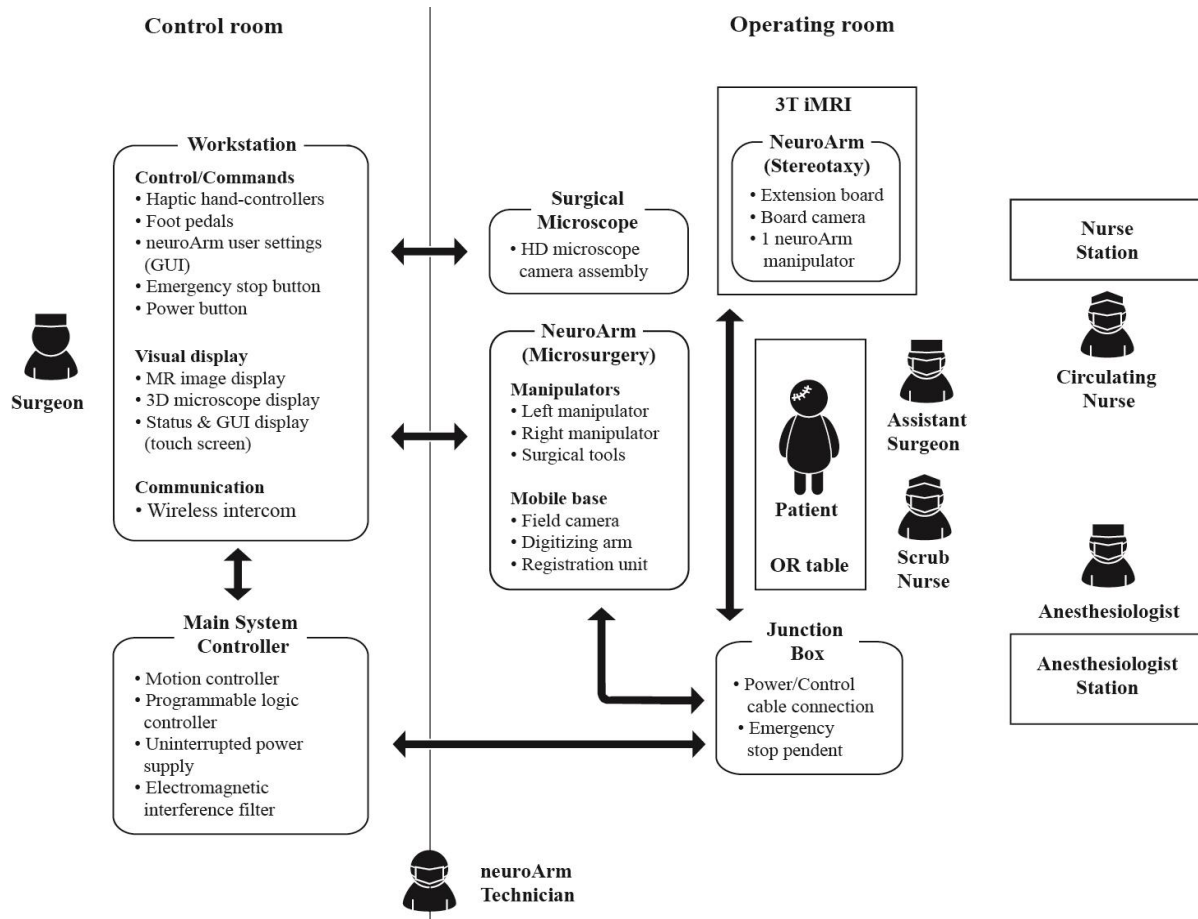


Fig. 3. Overview of the neuroArm system components and clinical setup at the operating suite during robotic surgery. Control and power signals are sent/received to/from the workstation and main system controller via a junction box located in the OR, underneath the OR table.

2. 4. Master-Slave Mapping System

Schematic of the neuroArm manipulator and its active joints (DOFs) are shown in Fig. 4. The DOFs are: shoulder yaw (θ_1), shoulder roll (θ_2), elbow yaw (θ_3), elbow roll (θ_4), wrist pitch (θ_5) and tool roll (θ_6). The workspace of each manipulator is recognized by three translations with respect to the reference frame (P_x^L, P_y^L, P_z^L for left one or P_x^R, P_y^R, P_z^R for right one) and three orientations about the axes of reference frame, ($\gamma^{L/R}, \theta^{L/R}$ and $\phi^{L/R}$). The reference frame is shown with $\{x_s \ y_s \ z_s\}$. To control the position and

orientation of each manipulator, the differential motion of corresponding hand-controller is mapped to the differential motion of that manipulator.

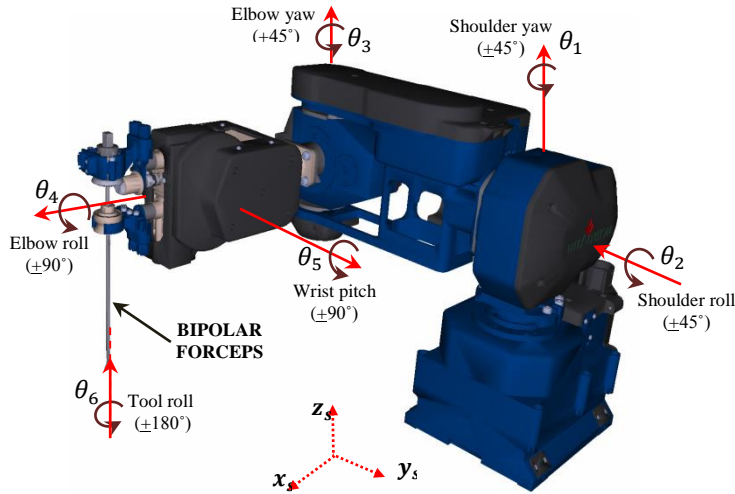


Fig. 4. Diagram of active joints in right neuroArm manipulator to which the bipolar forceps is attached.

3. Clinical Case Study

The results are taken from a grade III oligoastrocytoma surgical procedure performed by the neuroArm surgical system. Data were collected over 250 seconds. There were three main tasks considered by the surgeon: tissue manipulation, bipolar coagulation of tissues, and object placement such as cotton strips. In all these tasks, the surgeon at the work-station utilized two haptic devices (hand-controllers) to control the motion of each tool at the robotic end-effector, bipolar forceps on the right and suction tool on the left.

4. Results

4. 1. Linear Displacement of Surgical Tools

Positions of the bipolar forceps tip and suction tip recorded over 250 seconds of surgery are illustrated in Figs. 6 and 7. For this typical case, the ranges of the right end-effector (forceps tip) motion were 17.4 mm, 17.9 mm, and 16.1 mm along the reference frame (x_s , y_s , and z_s axes). On the other hand, the left end-effector (suction tip) travelled by 18.1 mm, 28.7 mm and 22.2 mm along x_s , y_s , and z_s axes, respectively. Table 1 presents mean positions \pm the standard error of the mean (\pm SEM) of the bipolar forceps and the suction during 250 seconds of surgery. As observed, in order to perform this case of operation, over the investigated time interval, the bipolar forceps needs to displace by $17.4 \times 17.9 \times 16.1$ mm along x_s , y_s , and z_s axes, and the suction requires $18.1 \text{ mm} \times 28.7 \text{ mm} \times 22.2 \text{ mm}$ workspace to move. Note that, the standard error of the mean (\pm SEM) takes into account both the standard deviation (SD) value and the sample size.

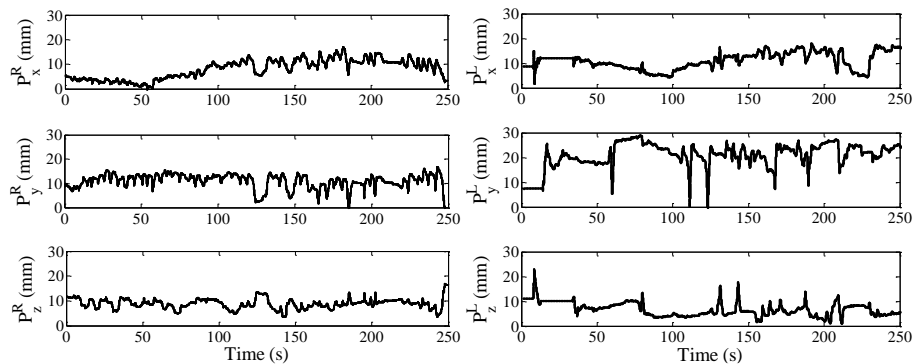


Fig. 5. Linear displacement of the forceps (P^R) and the suction (P^L) end-effectors along three axes.

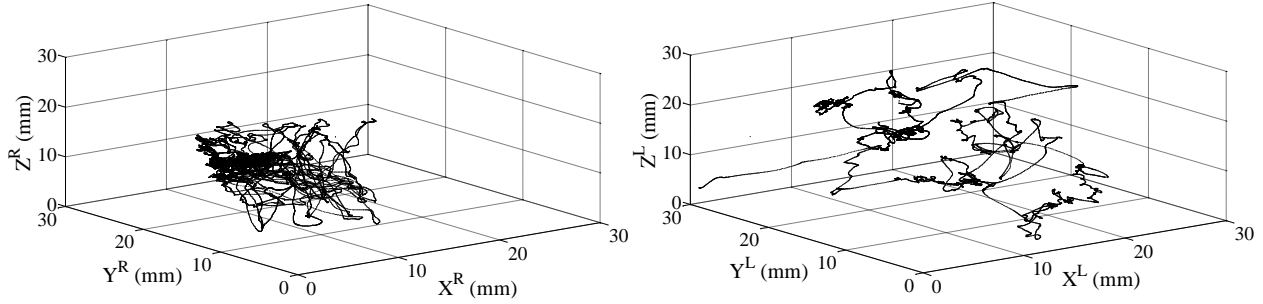


Fig. 6. 3D view of positions of the bipolar forceps (\cdot^R) and the suction (\cdot^L) tips during surgery.

Table 1. Linear and angular displacements of the right and left end-effector over 250 seconds of surgery.

Variable	Bipolar forceps		Suction	
	Mean value \pm SEM (mm, $^\circ$)	Position interval (mm, $^\circ$)	Mean value \pm SEM (mm, $^\circ$)	Position interval (mm, $^\circ$)
P_x	6.89 ± 0.11	[0, 17.4]	8.65 ± 0.06	[0, 18.1]
P_y	8.02 ± 0.14	[0, 17.9]	11.30 ± 0.05	[0, 28.7]
P_z	6.12 ± 0.12	[0, 16.1]	8.97 ± 0.08	[0, 22.2]
γ	9.9 ± 0.11	[0, 17.6]	6.7 ± 0.05	[0, 16.8]
θ	4.1 ± 0.09	[0, 10.2]	8.3 ± 0.05	[0, 18.1]
φ	11.2 ± 0.13	[0, 20.0]	5.8 ± 0.04	[0, 13.3]

4. 2. Angular Displacement of Surgical Tools

Figure 7 presents variations of orientation components in the bipolar forceps at the right manipulator and suction, at the left manipulator. As observed, the forceps tool oriented by 17.6° , 10.2° and 20.0° about x_s , y_s , and z_s axes, respectively. The suction also had the orientation range of 16.8° (about x_s), 18.1° (about y_s), and 13.3° (about z_s). The orientation components of both surgical tools are listed in Table 1. As seen in Figs. 5 and 7, the position and orientation of the forceps are more oscillatory than the suction that could be because of performing different tasks by the forceps while the suction does a single task.

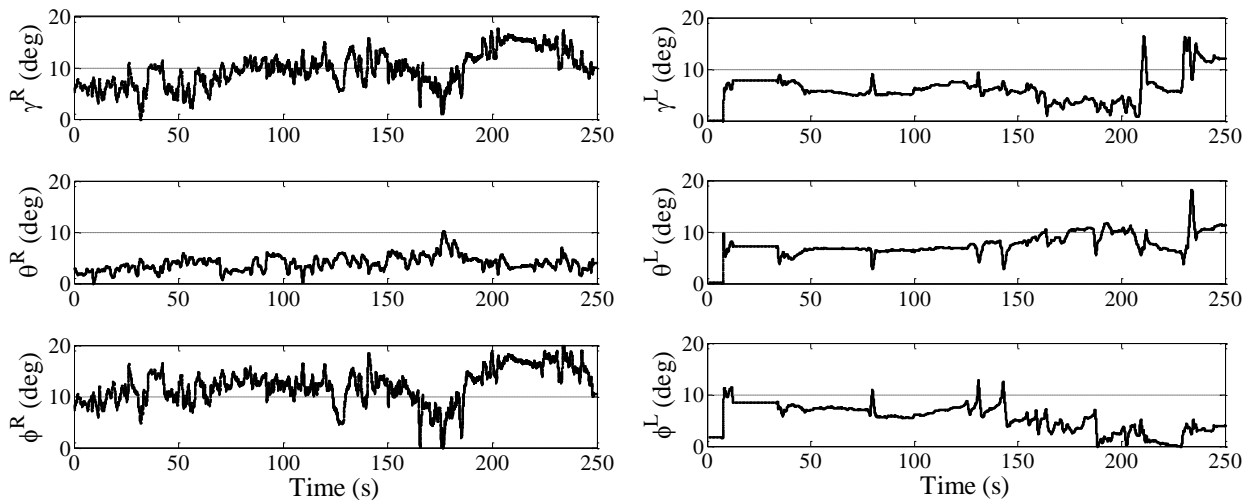


Fig. 7. Angular displacement of the bipolar forceps (\cdot^R) and the suction (\cdot^L) tips over 250 seconds of neurosurgery.

4. 3. Interaction Forces

Figure 8 illustrates total force exerted over time, $F = (F_x^2 + F_y^2 + F_z^2)^{1/2}$, for the surgical case presented in Figs. 5 and 7. For this experiment, the mean values (\pm SEM) of the total forces at the bipolar forceps and suction tips were $F^R = 0.39 \pm 0.06$ N and $F^L = 0.18 \pm 0.04$ N, respectively. Moreover, the maximum value of the measured force, at either right or left end-effector, was 1.26 N. As observed, the value of forces at the bipolar forceps is greater than the suction. Results, given in Fig. 8, are the modified versions of the forces in which the offset forces, resulted from initial installation of the surgical tools, have been subtracted from the measured force by the force sensor. Table 2 presents the mean values (\pm SEM) of interaction forces at both right and left manipulator end-effectors. As shown, the mean value of measured forces at the suction tip was less than the bipolar forceps side. Moreover, the oscillations (and the SEM values) of force signal in the forceps is more than the ones in the suction.

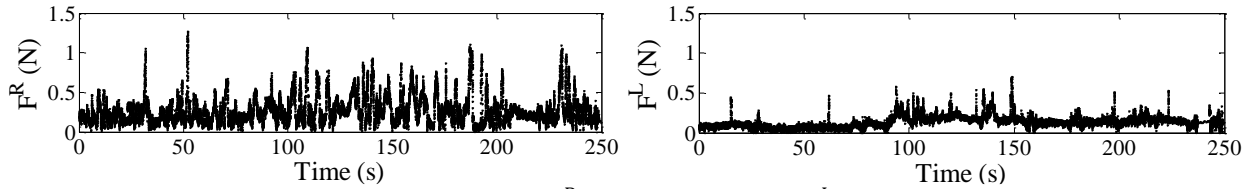


Fig. 8. Total force at the bipolar forceps tip (F^R) and the suction tip (F^L) measured by the force sensor.

Table 2. Force components of both surgical tools over 250 seconds of surgery.

Variable	Bipolar forceps	Suction	Peak force (N)
	Mean value \pm SEM (N)	Mean value \pm SEM (N)	
F_x	0.16 ± 0.02	0.08 ± 0.01	0.98
F_y	0.19 ± 0.01	0.09 ± 0.01	1.09
F_z	0.21 ± 0.04	0.11 ± 0.02	1.17
F	0.39 ± 0.06	0.18 ± 0.04	1.26

5. Conclusions

This paper reported the required workspace and tool-tissue interaction forces of surgical tools in a robot-assisted microsurgical resection of a grade III oligoastrocytoma. The surgery was performed using the neuroArm system located at the Foothills Hospital, University of Calgary. neuroArm consists of two manipulators that hold two surgical tools, attached to each robotic arm: in this case, a bipolar forceps on the right and a suction tool on the left. According to the studied case, it was shown that the forceps required a workspace of $17 \times 18 \times 16$ mm³ and offered absolute orientation ranges of 10°, 4° and 11° to conduct the surgery. Maximum tool-tissue interaction forces of 0.39 N and 0.18 N were recorded for the bipolar forceps and the suction, respectively. However, the position, orientation and force responses, over examined time interval, were more oscillatory for the bipolar forceps than the ones in the suction tool. Furthermore, the SEM values of these parameters were larger in the forceps than the suction. Ongoing and future work will focus on quantifying the force and workspace of the surgical tools in multiple patients with varying neurosurgical procedures. The work will not only provide valuable data relative to robot assisted surgery, but also can also provide useful quantitative data to assist in training of neurosurgical trainees.

References

- Arata J., Tada Y., Kozuka H., Wada T., Saito Y., Ikedo N., Hayashi Y., Fujii M., Kajita Y., Mizuno M., Wakabayashi T., Yoshida J., Fujimoto H. (2011). Neurosurgical Robotic System for Brain Tumor Removal. *Comput. Assist. Radiol. Surg.*, 6(3), 375-385.
- Camarillo D.B., Krummel T.M., Salisbury J.K. (2004). Robotic Technology in Surgery: Past, Present, and Future. *Am J. Surg.*, 188, 2S-15S.

- Comparettei M.D., Vaccarella A., De Lorenzo D., Ferrigno G., De Momi E. (2011). Multi-robotic Approach for Keyhole Neurosurgery: The ROBOCAST Project, *Proc. of Joint Workshop on New Technologies for Computer/Robot Assisted Surgery*, Austria.
- Gonzalez-Martinez J., Vadera S., Mullin J., Enatsu R., Alexopoulos A.V., Patwardhan R., Bingaman W., Najm I. (2014). Robot-Assisted Stereotactic Laser Ablation in Medically Intractable Epilepsy: Operative Technique. *Neurosurgery*, 10(2), 167-72.
- Goto T., Miyahara T., Toyoda K., Okamoto J., Kakizawa Y., Koyama J.I., Fujie M. G., Hongo K. (2009). Telesurgery of Microscopic Micromanipulator System “NeuRobot” in Neurosurgery: Interhospital Preliminary Study. *Cent. Nerv. Syst. Dis.*, 2009(1), 45-53.
- Greer A.D., Newhook P., Sutherland G.R. (2006). Human-Machine Interface for Robotic Surgery and Stereotaxy. *Computer Assisted Radiology and Surgery*, 1, 295-297.
- Haidegger T., Tian X., Kazanzides P. (2008). Accuracy Improvement of a Neurosurgical Robot System, *Proc. Of IEEE Int. Conf. on Biomedical Robotics and Biomechatronics*, Scottsdale, USA, 836-841.
- Hongo K., Goto T., Miyahara T., Kakizawa Y., Koyama J., Tanaka Y. (2006). Telecontrolled Micromanipulator System (NeuRobot) for Minimally Invasive Neurosurgery. *ACTA Neurochir. Suppl.*, 98, 63-66.
- Maddahi Y., Rahman R.A., Fung W.K., Sepehri N. (2013). Effect of Network Quality on Performance of Bilateral Teleoperated Hydraulic Actuators: A Comparative Study. *Control and Intelligent Systems*, 41(1), 11-25.
- Marcus H.J., Zareinia K., Gan L.S., Yang W.F., Lama S., Guang-Zhong Yang G.Z., Sutherland G.R. (2014). Forces Exerted During Microneurosurgery: A Cadaver Study. *Medical Robotics and Computer Assisted Surgery*, 10(9), 251-256.
- Mitsuishi M., Morita A., Sugita N., Sora S., Mochizuki R., Tanimoto K., Baek Y.M., Takahashi H., Harada K. (2013). Master-slave Robotic Platform and its Feasibility Study for Micro-Neurosurgery, *Int. J. Med. Robot.*, 9(2), 180-189.
- Shoham M., Brink-Danan S., Friedlander A., Knoller N. (2006). Bone-mounted Miniature Robotic System for Spine Surgery, *Proc. of IEEE Int. Conf. on Biomedical Robotics and Biomechatronics*, Piscataway, USA, 4.
- Sutherland G.R., McBeth P.B., Louw D.F. (2003). NeuroArm: An MR Compatible Robot for Microsurgery, *International Congress Series*, 1256, 504–508.
- Sutherland G.R., Newhook P., Feil G., Fielding T., Greer A.D., Latour I. (2008a). An Image-Guided MR Compatible Surgical Robot. *Neurosurgery*, 62, 286-293.
- Sutherland G.R., Latour I., Greer A.D. (2008b). Integrating an Image Guided Robot with Intraoperative MRI: A Review of Design and Construction. *IEEE Engineering in Medicine and Biology*, 27, 59-65.
- Sutherland G.R., Lama S., Gan L.S., Wolfsberger S., Zareinia K. (2013). Merging Machines with Microsurgery: Clinical Experience with neuroArm. *Neurosurgery*, 118(3), 521-529.
- Sutherland G.R., Maddahi Y., Gan L.S., Lama S., Zareinia K. (2015). Robotics in the Neurosurgical Treatment of Glioma. *Surgical Neurology International Supplement*, 6(S2), 1-8.
- Zareinia K., Maddahi Y., Ng C., Sepehri N., Sutherland G.R. (2015). Performance Evaluation of Haptic Hand-Controllers in a Robot-Assisted Surgical System. *International Journal of Medical Robotics and Computer Assisted Surgery*.